Research Article | Vol. 25, No. 16 | 7 Aug 2017 | OPTICS EXPRESS 19281
Optics EXPRESS

Coherent beam combining and noise analysis of a colliding pulse modelocked VECSEL

SANDRO M. LINK,* DOMINIK WALDBURGER, CESARE G. E. ALFIERI, MATTHIAS GOLLING, AND URSULA KELLER

Department of Physics, Institute for Quantum Electronics, ETH Zürich, 8093 Zürich, Switzerland
**slink@phys.ethz.ch*

Abstract: Optically-pumped SESAM-modelocked semiconductor disk lasers have become interesting ultrafast lasers with gigahertz pulse repetition rates, high average power and adjustable lasing wavelength. It is well established that colliding pulse modelocking (CPM) can generate both shorter pulses and improved stability. These improvements however typically come at the expense of a more complex ring cavity and two output beams. So far similar modelocking results have been obtained with CPM vertical external-cavity surface-emitting lasers (VECSELs) and with SESAM-modelocked VECSELs or modelocked integrated external-cavity surface-emitting lasers (MIXSELs) in a linear cavity. However coherent beam combining of the two output beams of a CPM VECSEL could result in a significantly higher peak power. This is interesting for example for applications in biomedical microscopy and frequency metrology. Here we demonstrate with a more detailed noise analysis that for both output beams of a CPM VECSEL the pulse repetition rates and the carrier envelope offset frequencies are locked to each other. In contrast to standard SESAM-modelocked VECSELs in a linear cavity, we only have been able to actively stabilize the pulse repetition rate of the CPM VECSEL by cavity length control and not by pump-power control. Furthermore, a first coherent beam combining experiment of the two output beams is demonstrated.

OCIS codes: (140.4050) Mode-locked lasers; (140.5960) Semiconductor lasers; (140.3560) Lasers, ring; (140.3298) Laser beam combining; (140.3425) Laser stabilization.

References and links

1. R. L. Fork, B. I. Greene, and C. V. Shank, "Generation of optical pulses shorter than 0.1 ps by colliding pulse modelocking," Appl. Phys. Lett. **38**(9), 617–619 (1981).
2. G. H. C. New, "Modelocking of quasi-continuous lasers," Opt. Commun. **6**(2), 188–192 (1972).
3. J. A. Valdmanis and R. L. Fork, "Design Considerations for a Femtosecond Pulse Laser Balancing Self Phase Modulation, Group Velocity Dispersion, Saturable Absorption, and Saturable Gain," IEEE J. Quantum Electron. **22**(1), 112–118 (1986).
4. Y. K. Chen, M. C. Wu, T. Tanbun-Ek, R. A. Logan, and M. A. Chin, "Subpicosecond monolithic colliding-pulse modelocked multiple quantum well lasers," Appl. Phys. Lett. **58**(12), 1253–1255 (1991).
5. Y.-K. Chen and M. C. Wu, "Monolithic Colliding Pulse Modelocked Quantum Well Lasers," IEEE J. Quantum Electron. **28**(10), 2176–2185 (1992).
6. A. Laurain, D. Marah, R. Rockmore, J. McInerney, J. Hader, A. R. Perez, W. Stolz, and J. V. Moloney, "Colliding pulse mode locking of vertical-externalcavity surface-emitting laser," Optica **3**(7), 781–784 (2016).
7. A. Laurain, R. Rockmore, H. T. Chan, J. Hader, S. W. Koch, A. R. Perez, W. Stolz, and J. V. Moloney, "Pulse interactions in a colliding pulse mode-locked vertical external cavity surface emitting laser," J. Opt. Soc. Am. B **34**(2), 329–337 (2017).
8. B. W. Tilma, M. Mangold, C. A. Zaugg, S. M. Link, D. Waldburger, A. Klenner, A. S. Mayer, E. Gini, M. Golling, and U. Keller, "Recent advances in ultrafast semiconductor disk lasers," Light Sci. Appl. **4**, e310 (2015).
9. M. A. Gaafar, A. Rahimi-Iman, K. A. Fedorova, W. Stolz, E. U. Rafailov, and M. Koch, "Mode-locked semiconductor disk lasers," Adv. Opt. Photonics **8**(3), 370–400 (2016).
10. D. Waldburger, S. M. Link, M. Mangold, C. G. E. Alfieri, E. Gini, M. Golling, B. W. Tilma, and U. Keller, "High-power 100 fs semiconductor disk lasers," Optica **3**(8), 844–852 (2016).
11. D. J. H. C. Maas, A.-R. Bellancourt, B. Rudin, M. Golling, H. J. Unold, T. Südmeyer, and U. Keller, "Vertical integration of ultrafast semiconductor lasers," Appl. Phys. B **88**(4), 493–497 (2007).

#296570 https://doi.org/10.1364/OE.25.019281
Journal © 2017 Received 21 Jun 2017; revised 18 Jul 2017; accepted 22 Jul 2017; published 1 Aug 2017

Optics EXPRESS

12. C. G. E. Alfieri, D. Waldburger, S. M. Link, E. Gini, M. Golling, G. Eisenstein, and U. Keller, "Optical efficiency and gain dynamics of modelocked semiconductor disk lasers," Opt. Express **25**(6), 6402–6420 (2017).
13. M. Mangold, S. M. Link, A. Klenner, C. A. Zaugg, M. Golling, B. W. Tilma, and U. Keller, "Amplitude noise and timing jitter characterization of a high-power mode-locked integrated external-cavity surface emitting laser," IEEE Photonics J. **6**(1), 1–9 (2014).
14. S. M. Link, D. J. H. C. Maas, D. Waldburger, and U. Keller, "Dual-comb spectroscopy of water vapor with a free-running semiconductor disk laser," Science **356**(6343), 1164–1168 (2017).
15. F. F. Voigt, F. Emaury, P. Bethge, D. Waldburger, S. M. Link, S. Carta, A. van der Bourg, F. Helmchen, and U. Keller, "Multiphoton in vivo imaging with a femtosecond semiconductor disk laser," Biomed. Opt. Express **8**(7), 3213–3231 (2017).
16. A. Klenner, A. S. Mayer, A. R. Johnson, K. Luke, M. R. E. Lamont, Y. Okawachi, M. Lipson, A. L. Gaeta, and U. Keller, "Gigahertz frequency comb offset stabilization based on supercontinuum generation in silicon nitride waveguides," Opt. Express **24**(10), 11043–11053 (2016).
17. H. R. Telle, G. Steinmeyer, A. E. Dunlop, J. Stenger, D. H. Sutter, and U. Keller, "Carrier-envelope offset phase control: A novel concept for absolute optical frequency measurement and ultrashort pulse generation," Appl. Phys. B **69**(4), 327–332 (1999).
18. S. M. Link, A. Klenner, and U. Keller, "Dual-comb modelocked lasers: semiconductor saturable absorber mirror decouples noise stabilization," Opt. Express **24**(3), 1889–1902 (2016).
19. T. M. Shay, V. Benham, J. T. Baker, A. D. Sanchez, D. Pilkington, and C. A. Lu, "Self-synchronous and self-referenced coherent beam combination for large optical arrays," IEEE J. Sel. Top. Quantum Electron. **13**(3), 480–486 (2007).
20. T. W. Hänsch and B. Couillaud, "Laser frequency stabilization by polarization spectroscopy of a reflecting reference cavity," Opt. Commun. **35**(3), 441–444 (1980).

1. Introduction

Colliding pulse modelocking (CPM) was first introduced with passively modelocked dye lasers [1]. The modelocking is based on dynamic gain saturation for which a critical balance between loss and gain saturation opens up a net gain window [2]. Better modelocking stability and shorter pulses were achieved with a ring laser when the distance between the absorber and the gain is about one quarter of the resonator roundtrip length. In this case, the two pulses propagating in opposite direction collide in the saturable absorber and saturate the absorber more strongly. In addition, the time between the pulses in the gain corresponds to half the roundtrip time which allows for the gain to recover to the same value for both pulses. The optimization of the CPM Rhodamine 6G laser resulted in world-record pulse durations of only 27 fs [3]. The CPM technique then has been also applied for semiconductor lasers with a monolithic edge-emitting quantum well laser in a linear cavity [4, 5]. However, the critical cavity stability requirements seem to have prevented a stronger impact of this approach so far. More recently the CPM technique has been used for an optically pumped vertical-external cavity surface-emitting laser (VECSEL) in a ring cavity [6] generating pulses as short as 128 fs with an average power of 90 mW per output beam at a pulse repetition rate of 3.27 GHz [7].

However, it is not clear that the additional complexity of a ring cavity is justified when we compare CPM VECSELs with standard SESAM-modelocked VECSELs [8, 9]. Stable modelocking with pulses as short as 96 fs with 100 mW of output power in a more simple linear cavity has been demonstrated [10]. In addition, CPM is not possible with the more compact approach of a modelocked integrated external-cavity surface-emitting laser (MIXSEL) [11] integrating the saturable absorber and the gain within the same semiconductor wafer. To date with optically pumped MIXSELs pulses as short as 184 fs with 115 mW average output power have been demonstrated [12]. The MIXSEL also provides a very stable optical frequency comb even without any further active stabilizations: for example a free-running single 2-GHz MIXSEL comb has a comb line spacing variation of only $\approx 2.5\ 10^{-4}$ integrated over a measurement time of 10 ms [13]. Such excellent modelocking stability enabled dual comb spectroscopy in water vapor with only one laser cavity and without any further active stabilization [14].

A CPM VECSEL has two output beams and so far it has not been demonstrated that these two beams are fully coherent and potentially could be combined to obtain a higher peak

Optics EXPRESS

power. This could be interesting for applications in biomedical microscopy [15] and supercontinuum generation [16]. Coherent beam combining requires that both the pulse repetition frequencies and the carrier envelope offset (CEO) frequencies [17] are identical for both beams, which has not been demonstrated for CPM VECSELs to date. Here, we analyze the noise behavior of a CPM VECSEL and confirm that indeed, both the pulse repetition frequencies and the CEO frequencies of both beams are intrinsically locked to each other. We coherently combine the two beams in a proof-of-principle second harmonic generation (SHG) experiment.

2. Laser setup

The details of the VECSEL chip used to build the ring cavity can be found in [10]. The cavity comprises the VECSEL chip, the SESAM, a flat high reflectance mirror and an output coupler (OC) with 1% transmission and a radius of curvature of 100 mm [Fig. 1]. The total cavity length is 180 mm. Since there is no direction-selective element in the ring cavity, two pulses can propagate in opposite direction around the ring cavity. The CPM technique introduces a stronger saturation of the saturable absorber based on interference of the two counter-propagating beams. This intrinsically favors the same linear polarization for both output beams which was also observed in our experiment. However, depending on the pump power, we have observed that both beams can simultaneously switch from p- to s-polarization. This was also observed in the linear cavity configuration using the same VECSEL chip. Since part of the experiment is polarization sensitive such as the second harmonic crystal, we introduced an intracavity Brewster plate to fix the polarization. For the distance between the VECSEL chip and the SESAM ($L_{V\text{-}S}$) a quarter of the total cavity length is chosen to enable an equal pumping duration and gain recovery time for both counter-propagating pulses [6].

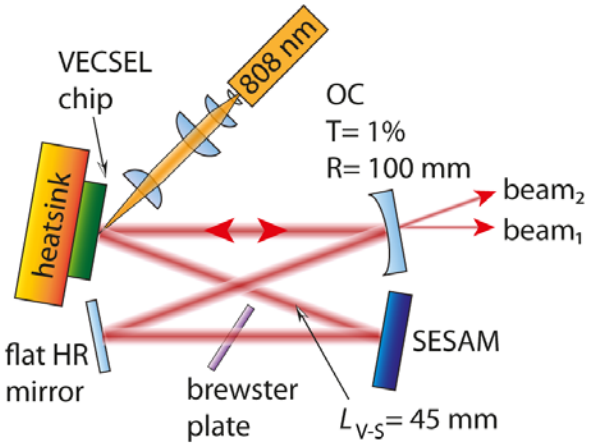

Fig. 1. Colliding pulse modelocked (CPM) VECSEL. The VECSEL chip is optically pumped by a cw 808-nm diode laser array. The ring cavity enables two pulses propagating in opposite directions. Stable CPM is obtained when the cavity length between the VECSEL chip and the SESAM ($L_{V\text{-}S}$) is a quarter of the total cavity roundtrip length. OC, output coupler; HR, high reflector.

The VECSEL chip and the SESAM are operated at 20°C and 18°C, respectively. The cavity and pump spot on the gain chip have a beam radius of 177 µm and the beam radius on the SESAM is 100 µm. With a total pump power of 20 W, we achieved 170 mW average output power per beam. The diagnostics show that both beams have identical modelocking characteristics [Fig. 2]. The center wavelength of both beams is 1034.3 nm with a full width at half maximum (FWHM) of 2.4 nm [Fig. 2(a)]. The pulse duration, measured with a

Optics EXPRESS

second-harmonic autocorrelation, is for both beams 780 fs [Fig. 2(b)] and the pulse repetition frequencies are identical with 1.668 GHz, shown for the full span of the microwave spectrum analyzer (MSA) of 13 GHz with a resolution bandwidth (RBW) of 30 kHz [Fig. 2(c)] and magnified around the first harmonic in a span of 10 MHz with a RBW of 1 kHz [Fig. 2(d)]. The goal of this experiment was not to obtain a new record performance of CPM VECSELs but to study the coherence of the two output beams and investigate if coherent beam combining is possible. Therefore, we did not optimize the CPM VECSEL for short pulse durations but used a very stable configuration at room temperature that delivered reproducible parameters over weeks of operation.

3. Pulse repetition frequency analysis

In CPM operation both pulses collide in the SESAM. Constructive interference of the two pulses increases the saturation of the SESAM which is energetically favorable. Therefore we expect that CPM locks the pulse repetition rates of the two counter-propagating beams. We recently observed similar intrinsic locking in case of a dual-comb modelocked SDL with sufficient spatial and temporal overlap on the absorber [18]. However, the microwave spectrum measurement of the pulse repetition frequency [Fig. 2(d)] is not sufficient as proof for perfectly synchronized pulses, since small asynchronous timing jittering would not be resolved with an MSA measurement.

We actively stabilize the pulse repetition frequency of one of the two beams ($beam_1$) by actively controlling the cavity roundtrip length. We then measure the phase noise of both beams with a signal source analyzer (SSA) [Fig. 3]. For this stabilization approach we detect the pulse repetition frequency of $beam_1$ with a photodetector and mix the signal with a low noise electronic reference set to the same frequency. The phase error of the mixed signal is fed to a phase-locked loop (PLL). We exchanged the half-inch output coupler with a 2-mm thick output coupler that we mount on a piezo actuator. By sending the correction voltage of

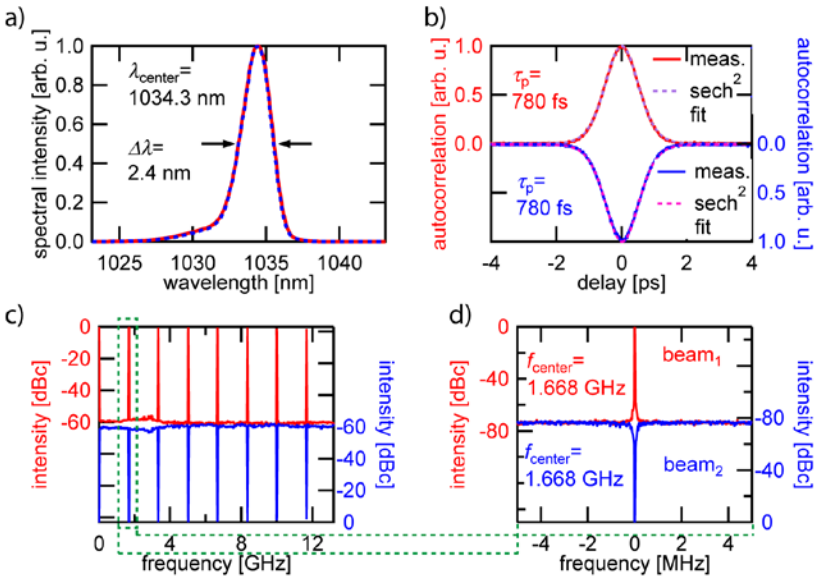

Fig. 2. CPM VECSEL modelocking results for the two output beams: $beam_1$ (red) and $beam_2$ (blue). a) The optical spectrum is identical for both beams. b) Second harmonic autocorrelations show for each beam a pulse duration of 780 fs. c) Microwave spectrum measured over the full span of the microwave spectrum analyzer with a resolution bandwidth (RBW) of 30 kHz. d) Microwave spectrum zoomed in around the first harmonic with a span of 10 MHz and a RBW of 1 kHz confirms that both beams have the same pulse repetition frequency.

Optics EXPRESS

the PLL to the piezo, the cavity length is actively changed to compensate for the phase error. With a second photodetector, we measure the phase noise of $beam_1$ out-of-loop with the SSA. A strong reduction of the phase noise of over 100 dB is observed from free-running to stabilized operation [Fig. 3]. We keep the stabilization of $beam_1$ active and measure the phase noise of $beam_2$. Also for the pulse repetition frequency of $beam_2$ the phase noise is reduced by the same amount [Fig. 3], confirming that both pulse repetition rates are fully locked.

In CPM the intrinsic lock of the pulse repetition rate is based on the colliding pulses on the saturable absorber which is a pulse-energy dependent and interferometric mechanism. Thus, stabilization via the cavity length is an independent feedback mechanism. To investigate further, we also try to stabilize the pulse repetition frequency of $beam_1$ by modulating the current of the pump diode instead of the cavity length. All other parts of the detection and the PLL remain unchanged. *In this configuration, it is not possible to lock the phase noise*. We did try to stabilize the CPM laser via pump-power modulation under different operation parameters such as cooling temperatures, pump power levels and cavity lengths, but still no locking was achieved.

Previously without CPM we stabilized the pulse repetition frequency of a standard SESAM-modelocked VECSEL via both cavity length and pump-power control and obtained the same stabilization performance. However, the pump power modulation changes the pulse energy and therefore starts to affect the CPM. The effect is so strong that no active stabilization of the pulse repetition rate is possible with pump-power control any more.

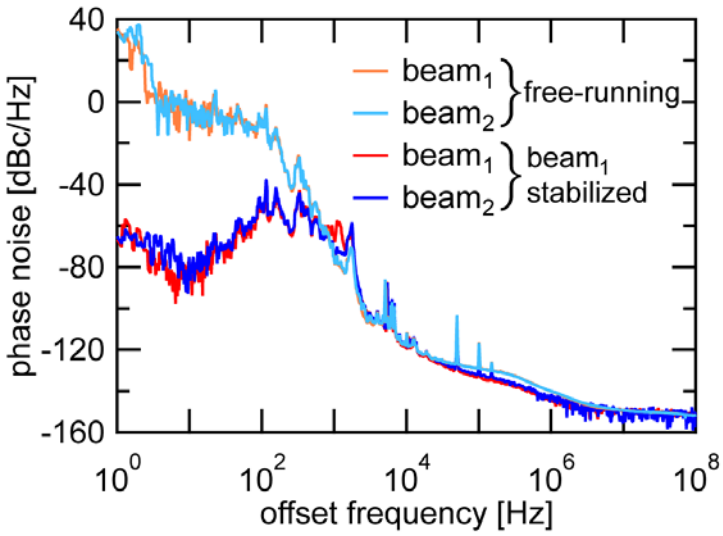

Fig. 3. Phase noise measurements of the pulse repetition frequencies of the two output beams from the CPM VECSEL. If the pulse repetition frequency of $beam_1$ is actively stabilized by controlling the cavity roundtrip time, the noise is drastically reduced for both beams simultaneously, confirming that the two pulse repetition frequencies are locked with CPM. Note that it was not possible to obtain the same stabilization by controlling the pump power.

4. Carrier envelope offset (CEO) frequency analysis

For coherent beam combining we need a fully locked frequency comb with both a locked pulse repetition frequency and a carrier envelope offset (CEO) frequency. For the following analysis of CEO frequencies, the pulse repetition frequency is not stabilized. Assuming the two CEO frequencies in each output beam are different but relatively stable with respect to each other, we should be able to detect the difference in CEO frequency as a beat signal on a photodetector. We obtain both a spatial and temporal overlap of the two output beams in the same polarization with a delay stage in the path of $beam_2$ before the spatial combination of

Optics EXPRESS

the two beams with a 50:50 beam splitter (BS) [Fig. 4(a)]. The temporal overlap is confirmed by an autocorrelation measurement. However, no relative CEO beat frequency is visible in the microwave spectrum [Fig. 4(b)]. This means that either both CEO frequencies are identical or their relative noise is so high that the beat frequency stays below the noise floor of the MSA. To distinguish these two possibilities, we send $beam_2$ through an acousto-optic modulator (AOM) with a modulation frequency of 60 MHz [Fig. 4(c)]. We take the first diffraction order which introduces a frequency shift by 60 MHz for the full frequency comb of $beam_2$, resulting in an effective CEO frequency that is 60 MHz higher than before. If both CEO frequencies were the same, a relative beat signal should become visible at 60 MHz.

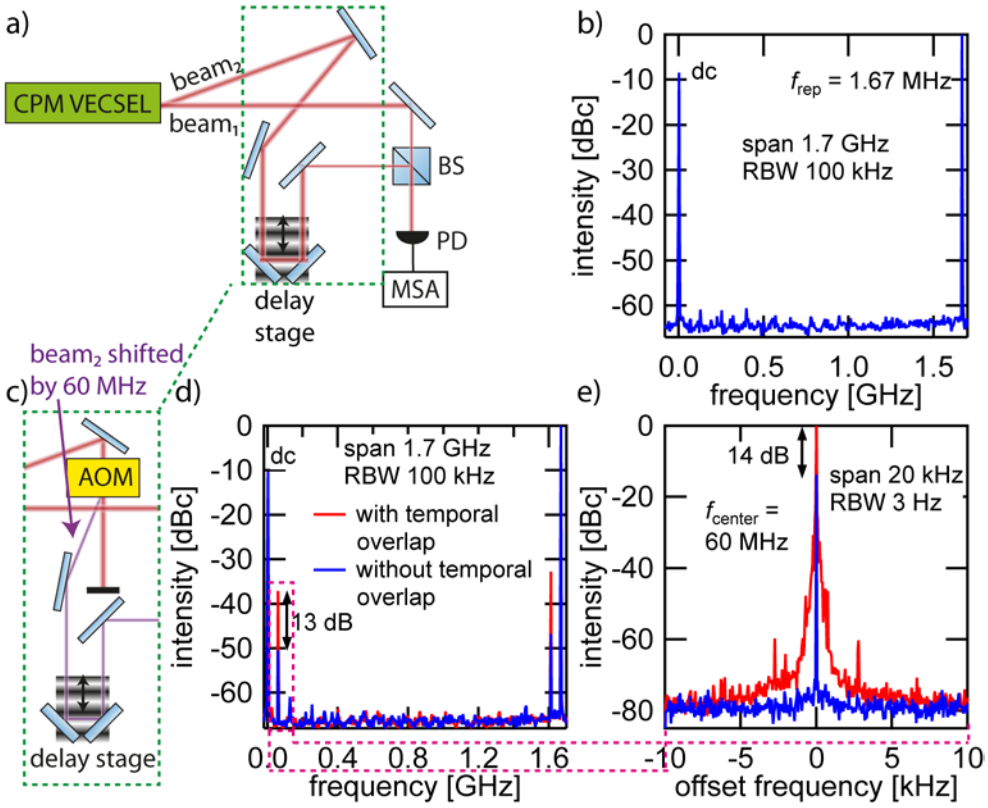

Fig. 4. Locked carrier envelope offset (CEO) frequencies of the two output beams from the CPM VECSEL: a) Setup to combine both beams with temporal overlap. BS, beams splitter; PD, photodetector; MSA microwave spectrum analyzer. b) The microwave spectrum shows no relative CEO beat frequency, maybe indicating that both CEO frequencies are identical. c) This is confirmed by shifting the frequency of $beam_2$ with an acousto-optic modulator (AOM) by 60 MHz and again combining the two beams with temporal overlap. d) CEO beat frequency is detected in the microwave spectrum at 60 MHz (red line) which is stronger than the peak coming from the radio frequency driver of the AOM that is also present without temporal overlap (blue line). e) Magnification of the microwave spectrum around the CEO beat frequency.

We combine the frequency-shifted $beam_2$ with $beam_1$ and measure the microwave spectrum. Without temporal overlap, there is already a signal detectable at 60 MHz. This signal comes from the strong radio frequency signal generated by the driver of the AOM and has a linewidth below the resolution of our MSA [blue line in Fig. 4(d), (e)]. When both beams are combined with temporal overlap, the beat signal at 60 MHz increases by 13 dB [red line in Fig. 4(d)]. The magnification of the CEO beat signal with a span of 20 kHz and a resolution bandwidth of 3 Hz shows a coherent peak of 23 dB on top of a noise pedestal of

Optics EXPRESS

roughly 1 kHz width [Fig. 4(e)]. The residual noise in the 1 kHz range is not caused by a difference in CEO of the two beams but is a result of the phase noise accumulated on the different paths of the beams, especially due to the mechanically not perfectly stable delay stage. We confirm the origin of the noise by splitting $beam_1$ with a beam splitter, sending one part through the AOM and the delay stage and then recombine it with the other part. The measured CEO beating shows the same noise pedestal, even though we beat the CEO frequency of $beam_1$ with itself, shifted by 60 MHz.

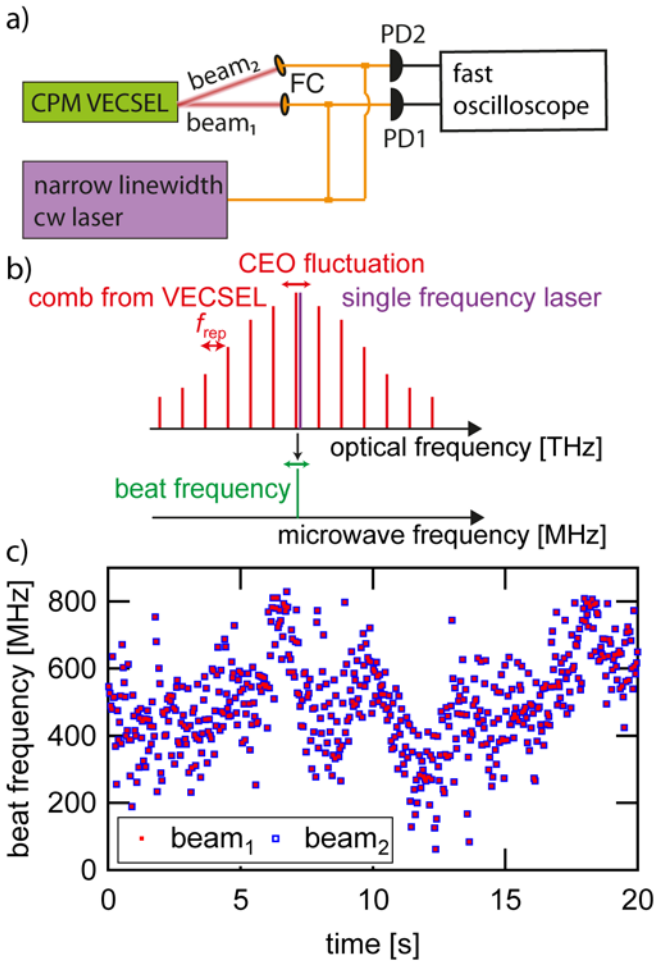

Fig. 5. Long-term CEO frequency fluctuations of the two output beams of the CPM VECSEL: a) Setup to detect the CEO frequency fluctuations of both beams simultaneously, by beating each comb with a narrow linewidth laser. FC, fiber coupling; PD photodetector. b) The interference between each comb of the VECSEL and the narrow linewidth laser generate a beat frequency, whose fluctuations are equal to the fluctuations of the CEO frequency of the VECSEL comb. Since we only want to observe, if both CEO frequencies fluctuate identically, we can ignore the fluctuations due to the pulse repetition frequency since we already confirmed that they are intrinsically locked with CPM. c) The perfectly synchronized fluctuations of the two beat frequencies are measured over 20 s with a gate time of 5 µs. Due to the calculation time of the Fourier transformation, the time between two measurements is 37 ms.

The measurement confirms that both CEO frequencies are identical, at least on a shorter time scale. To finally prove that they are perfectly locked also on a long time scale, we measure the CEO frequency of each beam simultaneously. This is realized by beating both

Optics EXPRESS

beams with a fiber-coupled single frequency laser (Toptica DLC CTL 1050). The wavelength of the single frequency laser is tuned to the center wavelength of the two beams and combined with each beam using fiber combiners [Fig. 5(a)]. Both beat signals are recorded simultaneously with a photodetector and a fast oscilloscope with 1 GHz bandwidth. The Fourier transformation of each time signal gives a frequency peak that fluctuates with the change of the CEO frequency of the corresponding beam [Fig. 5(b)]. Fluctuations of the pulse repetition frequency can be ignored since we have already confirmed in Section 3 that they are locked for both beams with CPM. We measure simultaneously the frequency fluctuations of the CEO frequency of each beam with a gate time of 5 µs [Fig. 5(c)]. The measurement shows clearly that both beat frequencies and therefore both CEO frequencies fluctuate in perfect synchronization. The large drifts of the CEO frequencies can be explained be the absence of any housing or shielding for the laser setup.

5. Coherent beam combining

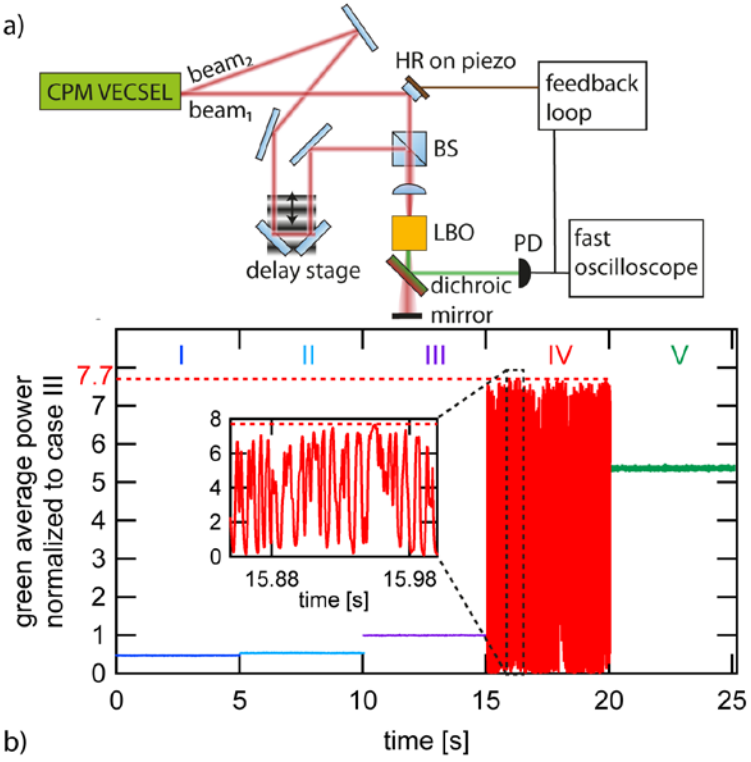

Fig. 6. Proof-of-principle experiment for coherent beam combining of the two output beams from the CPM VECSEL. a) Both beams are coherently combined and focused into a 20-mm long lithium triborate (LBO) crystal to generate green light through second harmonic generation. PD, photodetector; BS, beam splitter. b) The generated green light is measured with a PD and a fast oscilloscope for 5 different cases: (I): $beam_2$ is blocked and only half of the power of $beam_1$ arrives at the LBO crystal. (II): $beam_1$ is blocked and only half of the power of $beam_2$ arrives at the crystal. (III): half of the power of both beams arrive at the crystal without temporal overlap which is simply a incoherent superposition of the two intensities. (IV): both beams are coherently combined and interfere constructive and destructive. (V): the coherently combined signal is stabilized by changing the path-length difference with a with a feedback loop and a piezo actuator.

Since we have established that both beams of the CPM VECSEL have the same pulse repetition frequency and the same CEO frequency, all criteria for successful coherent beam combing of the two output beams are fulfilled. We test the coherent combination of the two

Optics EXPRESS

beams in a peak-power sensitive second harmonic generation (SHG) experiment. Both beams are combined with a beam splitter (BS) and the temporal overlap is controlled with the delay stage in one of the beam paths [Fig. 6(a)]. The beams are then focused into a lithium triborate (LBO) crystal of 20 mm length that was temperature stabilized at 184°C for non-critical phase matching. A dichroic mirror is used to separate the near infrared light at 1034 nm and the generated green light at 517 nm. The green light is measured with a photodetector and a fast oscilloscope.

If one of the beams is blocked, only half of the power of the other beam will go through the 50:50 BS and generate green [case I and II in Fig. 6(b)]. If both beams reach the BS but without temporal overlap, no interference occurs and half of the power of each beam will reach the crystal (case III). The power of the SHG signal scales with the square of the infrared pulse peak power. Therefore, without coherent combination the green signal in case III will be just the sum of the signals of case I and case II.

The situation drastically changes for case IV in [Fig. 6]: If the pulses of both beams arrive at the same time on the beam splitter, they interfere constructively or destructively, depending on the phase difference of the beams accumulated in their respective beam paths. For ideal constructive interference, all of the power of each beam will go through the BS and arrive simultaneously on the SHG crystal and the peak power will add up. This leads to an eight-fold stronger green generation compared to case III. Since the interference is phase sensitive, it varies from constructive to destructive within half a wavelength (517 nm) of path-difference of the two beams. The experimental setup was on the open table without housing or special care for mechanically stable mounts. This explains why the SHG green power signal fluctuates strongly in case IV. However, it reaches a maximum of 7.7, normalized to case III, which is very close to the ideal maximum of 8. The small difference to the ideal case can be explained by the fact that the power per beam reaching the BS was not identical and by the imperfection of the BS. The oscillation-periods of the green signal are mostly above 1 ms. This is confirmed by measuring the intensity noise of the SHG signal by taking the Fourier transformation of the signal in time [Fig. 7]. The noise drops to the noise floor in case IV above ≈1kHz, which is a typical value for mechanical noise and air disturbances. This also corresponds to the noise pedestal for the relative CEO frequency measurement [Fig. 4(e)], since the origin of the noise is the same.

The slow SHG power fluctuations with a bandwidth of 1 kHz can be compensated with a mirror mounted on a piezo actuator. The voltage signal of the green light in case IV is compared to a fixed voltage from a power supply. The error signal is fed to the same PLL used in section 3 and the correction voltage is send to a piezo actuator to control the path length of beam_1 [Fig. 6(a)]. With this method, we achieved a stabilized second harmonic signal at a level 5.3 times higher (case V) than in case III. With this simple stabilization method, it is not possible to stabilize the signal to the maximum level, since the error signal must be on the slope of the voltage signal. The intend is here to show that the coherently combined signal can be stabilized with little effort even in a setup not optimized for low-noise operation. With a more advanced detection scheme such as a lock-in amplification method [19] or the Hänsch-Couillaud method using a polarizing beam splitter [20], it is also possible to stabilize the coherently combined signal to the maximum value.

Optics EXPRESS

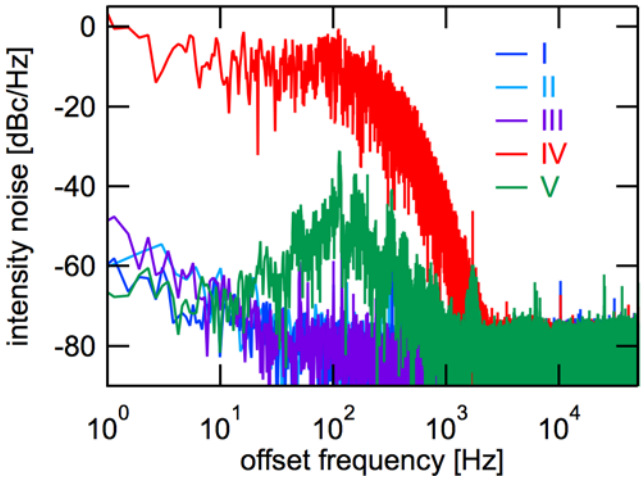

Fig. 7. Intensity noise of the second harmonic generation (SHG), calculated via Fourier transformation from the time-dependent power signal measured in [Fig. 6(b)] for the five different cases. The mechanical fluctuations changing the beam path difference in case IV show a bandwidth of ≈1 kHz before reaching the noise floor. They can be stabilized with a feedback loop and a piezo (case V).

6. Conclusion and outlook

We have realized colliding pulse modelocking (CPM) of a VECSEL-SESAM ring cavity. Our measurements show that both output beams have both identical pulse repetition frequencies and CEO frequencies. As expected from CPM we could only actively stabilize the pulse repetition rates of the two output beams with feedback over cavity length control and *not* with pump-power control. We can conclude that coherent beam combining of the two output beams is possible for further power scaling. We have demonstrated coherent beam combining in a proof-of-principle experiment with second harmonic generation.

For the current noise analysis experiments we did not optimize the VECSEL and the ring cavity for new world-record performance in terms of pulse duration and peak power. However, previously sub-200 fs pulses have been generated in such a CPM cavity configuration [7]. A coherent combination of the two beams has the potential to lead to a peak power of more than 1 kW, which should be sufficient to enable coherent supercontinuum generation in silicon nitride waveguides [16] and generate a self-referenced octave-spanning optical frequency comb from such a CPM VECSEL without any external pulse amplification. Other applications may also benefit from two output beams with identical frequency comb properties.

Funding

Swiss Confederation Program Nano-Tera.ch, which was scientifically evaluated by the Swiss National Science Foundation (SNSF).

Acknowledgments

The authors acknowledge support of the technology and cleanroom facility FIRST of ETH Zurich for advanced micro-and nanotechnology.